SAE International Journal of Commercial Vehicles, Vol. 10, Issue 2, 2017, Article number 2017-01-0425
DOI:10.4271/2017-01-0425

A Global Optimal Energy Management System for Hybrid Electric off-road Vehicles

Abstract—**Energy management strategies greatly influence the power performance and fuel economy of series hybrid electric tracked bulldozers. In this paper, we present a procedure for the design of a power management strategy by defining a cost function, in this case, the minimization of the vehicle's fuel consumption over a driving cycle. To explore the fuel-saving potential of a series hybrid electric tracked bulldozer, a dynamic programming (DP) algorithm is utilized to determine the optimal control actions for a series hybrid powertrain, and this can be the benchmark for the assessment of other control strategies. The results from comparing the DP strategy and the rule-based control strategy indicate that this procedure results in approximately a 7% improvement in fuel economy.**

Index Terms—**Series hybrid electric tracked vehicle, power management strategy, dynamic programming, rule-based**

I. INTRODUCTION

Construction vehicles, such as bulldozers, running on diesel engines serve an important role in modern societies with tremendous infrastructural development. The increasing reliance on construction vehicles brings certain negative impacts such as energy unsustainability and poor air quality. In recent years, hybrid electric vehicle (HEV) technology has been proposed as the technology for new bulldozer configurations. In the United States, Caterpillar produced the first D7E hybrid electric drive tracked bulldozer in March 2008. Compared to traditional models, CO and NOx emissions were reduced by approximately 10% and 20%, respectively. The D7E can improve fuel economy by 25%. In this briefing, a new hybrid electric tracked bulldozer composed of an engine-generator, two driving motors, and an ultracapacitor (UC) is put forward, and this bulldozer boasts high-efficiencies and less fuel consumption compared to traditional ones. The topology of the powertrain under study is the one presented in Fig.1. This hybrid electric tracked bulldozer uses an integrated controller to control two motors on both sides of the bulldozer independently and to transfer electric energy from the DC BUS into mechanical energy to drive the bulldozer. In this HEV, there are additional components, such as electric motors and an ultracapacitor, that provide more flexibility in the operation of the powertrain system to meet the driver's demand and minimize fuel consumption [1]. To fully realize the potential of the hybrid powertrain, the power management function of these vehicles must be carefully designed. By power management, we mean the development of a higher-level control algorithm that determines the total amount of energy to be generated, and this power management system uses two power sources. In other words, the power management control is implemented in the vehicle-level control system to coordinate the overall hybrid powertrain to satisfy certain performance targets such as fuel economy [2].

Energy management strategies for HEVs can be roughly classified into four categories [3]. The first type is the numerical optimization method, where the entire driving cycle is taken into consideration and the global optimization is found numerically, an example of this include dynamic programming [4],[5],[6], model predictive control [7], [8], and stochastic dynamic programming [9]. Optimization approaches rely on analytical or numerical optimization algorithms which are, obviously, able to optimize the performance. The second approach is the analytical optimization method including Pontryagin's minimum principle and the Hamilton-Jacobi-Bellmann equation [10]. The third type is the equivalent consumption minimization strategy (ECMS), which was introduced by Paganelli et al. [11] as an approach that determines the optimal power split at each time instant rather than over a time horizon [12],[13]. The fourth way employs heuristic control techniques such as control rules/ fuzzy logic/ neural networks for estimation and control algorithm development [14], [15]. Heuristic strategies depend on a set of rules to determine the control action at each time instant. The rules are designed in accordance with intuition, human expertise, and/or mathematical models and, usually, without prior knowledge of the driving information. The heuristic method is popular and has been successfully applied in commercial HEVs such as the Honda Insight and Toyota Prius. However, its major disadvantage is that the overall efficiency of the powertrain is not optimal, and the emission control is not directly considered.

In this article, we apply the dynamic programming (DP) algorithm to solve the optimal power management problem of a series hybrid electric tracked bulldozer. Differing from road vehicles, the HETB is one kind of tracked vehicle. Obviously, the mechanical property is different from that of the HEV. Apart from the structural differences between and HETB and HEV, their main difference lies in their working conditions. Unlike the HEV, the HETB's demand power changes dramatically between its soil-cutting stage and no-load stage under one certain drive cycle. Consequently, the MPC strategy's application in an HETB is more complicated than that in HEV. Furthermore, the drive cycle changes sharply according to the ground characteristic and even the weather condition in different working places. Thus, the MPC strategy's robustness is more important than that of HEV. Three scenarios were utilized to develop the energy management controller using the MPC. The first scenario is extracted from the typical working conditions of the bulldozer. The optimal solution over the typical drive cycle is obtained by minimizing the fuel consumption, and then, it is compared to the results gained from using a rule-based and DP power management strategies. As an approach that solves multi-step optimization problems based on Bellman's principle of optimality [16], DP provides a provably optimal energy management strategy through an

Published by SAE International. This is the Author Accepted Manuscript.
Please refer to any applicable publisher terms of use.

exhaustive search of all control and state grids. Applying DP in this series hybrid electric tracked bulldozer consists of finding the optimal control sequences to obtain the optimal ultracapacitor's state of energy (SOE) trajectory and to minimize fuel consumption over a given driving profile. However, exact knowledge of the driving profile is seldom known in practice [17]. Nonetheless, the DP provides a benchmark to assess the optimality of other energy management strategies and improve the online strategy [18], [19], [20].

The remainder of this paper is organized as follows: In Section II, The series hybrid electric tracked bulldozer (HETB) model is described. The dynamic optimization problem and the DP procedure of the optimal control problem for this series HETB is formulated in Section III. The optimal results for the fuel consumption case are given in Section IV, followed by conclusion and future work in Section V.

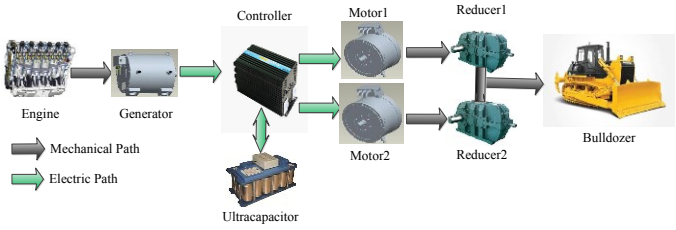

Fig. 1. The structure of the hybrid electric tracked bulldozer

II. Series HETB Powertrain Model

A. System Configuration

The baseline bulldozer studied here is the SD-24 tracked bulldozer of Shantui Construction Machinery Co., Ltd, and its powertrain configuration is shown in fig.1. The series hybrid power system is composed of a diesel engine, ultracapacitor, permanent magnet generator, motor drive system, and tracks. A 2.4F ultracapacitor was chosen as the energy storage system. The hybrid electric bulldozer uses the integrated controller to control the motors on both sides of the bulldozer independently and to transfer the electric energy from the generator and ultracapacitor into mechanical energy to drive the bulldozer. The hybrid electric tracked bulldozer model is implemented in SIMULINK. For more information of the model, the reader is referred to [21].

B. The Vehicle Model

The movement behavior of the bulldozer along its moving direction is completely determined by all of the forces that act on it in the same direction. Distinguishing it from an ordinary vehicle, the major external forces acting on the two tracks in the longitudinal direction include the external travel resistance F_E and the operating resistance F_T. The aerodynamic drag and the acceleration resistance are neglected since the velocity of the bulldozer is very low.

$$F_E = F_c + F_b = \frac{2b}{(n+1)k^{\frac{1}{n}}}\left(\frac{G}{2bL}\right)^{\frac{n+1}{n}} + \gamma Z^2 bK_\gamma + 2bZcK_{pc} \qquad (1)$$

$$\begin{aligned} F_T &= F_1 + F_2 + F_3 + F_4 \\ &= 10^6 B_1 h_p k_b + \frac{V\gamma\mu_1\cos\theta}{k_s} \\ &+ 10^6 B_1 X\mu_2 k_y + G_t\mu_2\cos\delta^2\cos\theta \end{aligned} \qquad (2)$$

where F_c is the compaction resistance (N); F_b is the bulldozing resistance (N); b is the track width (m); G is the vehicle weight (N); L is the track length (m); c is the soil cohesion coefficient (KPa); Ψ is the soil internal friction angle (º); n is the soil deformation index; k is the soil deformation modulus (KN/m^{n+2}); Z is the track amount of sinkage (m); γ is the unit weight (N/m^3); and N_γ and N_c are the soil Terzaghi coefficients of the bearing capacity [22]. F_1 is the soil-cutting resistance (N); F_2 is the pushing resistance of the mound before the blade (N); F_3 is the frictional resistance between the ground and blade (N); F_4 is the horizontal component of the frictional resistance when the soil rises along the blade (N); k_b is the cutting resistance per unit area (MPa); B_1 is the blade width (m); h_p is the average cutting depth (m); G_t is the gravity of the mound in front of the bulldozing plate; μ_1 is the friction coefficient between soil particles; μ_2 is the friction coefficient between the soil and blade; θ is the slope (°); V is the volume of the mound in front of the bulldozing plate; k_s is the loose degree coefficient of the soil; k_m is the fullness degree coefficient of the soil; H is the blade height (m); α_0 is the natural slope angle of the soil (°); k_y is the cutting resistance per unit area after the blade is pressed into the soil (MPa); X is the length of the worn blade contacting the ground (m); and δ is the cutting angle of the blade (°).

By combing Equations (1) and (2), the vehicle torque requirements for the powertrain, T_{req}, can be formulated as:

$$T_{req} = \frac{r}{i_0\eta}(F_E + F_T + m\dot{v}) \qquad (3)$$

Where, r is radius of the driving wheel; i_0 is the final gear ratio; η is the transmission efficiency; m is the vehicle mass; v is the vehicle drive speed along the longitudinal direction.

C. The Engine Model

Experimental data is used to generate the engine model. The fuel consumption map of the engine is expressed as the relationship between the crankshaft speed and power by a non-linear 3-D MAP constructed from experimental data as shown in Fig. 2.

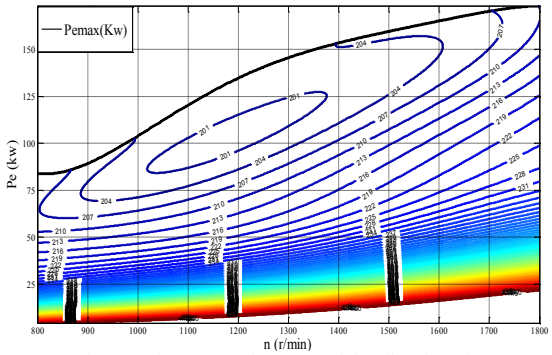

Fig.2 Fuel consumption map of the diesel engine

The engine map represents the fuel consumption as a function of the mechanical power and speed. Assuming that it is possible to control the engine in order to make it operate at the

fixed speed, the fuel consumption $\dot{B}_e$ (g/s) is a function only of the mechanical power delivered, P_e:

$$\dot{B}_e = \dot{B}_e(P_e) \tag{4}$$

The engine is constrained to operate within its limits:

$$\begin{aligned} &N_{e,\min}(t) \le N_e(t) \le N_{e,\max}(t); \\ &P_{e,\min}(t) \le P_e(t) \le P_{e,\max}(t); \\ &T_{e,\min}(t) \le T_e(t) \le T_{e,\max}(t); \end{aligned} \tag{5}$$

where N_e(t) is the engine speed at time t; $N_{e,\min}$(t) and $N_{e,\max}$(t) are the minimum and maximum speed of the engine at time t, respectively; P_e(t) is the output power of the engine at time t; $P_{e,\min}$(t) and $P_{e,\max}$(t) are the minimum and maximum output power of the engine at time t, respectively; T_e(t) is the engine torque at time t; and $T_{e,\min}$(t) and $T_{e,\max}$(t) are the minimum and maximum torque of the engine at time t, respectively.

D. The Generator and Motor Models

The generator and motor efficiency characteristics are expressed as a relationship between the speed and torque by a non-linear 3-D Map obtained from experimental data. The motor efficiency η_m at the operation point (n_m, T_m) is obtained from the following interpolation function:

$$\eta_m(n_m, T_m) = f(n_m, T_m) \tag{6}$$

where n_m is the speed of the motor, and T_m is the motor output torque.

E. The Ultracapacitor Model

The ultracapacitor pack is composed of several cells in both series and parallel modes. Each cell can be represented as a capacitance in series with a resistor. The capacitance models the ion accumulation; whereas, the resistance accounts for the electrolyte losses. The entire pack can be modeled by:

$$P_{uc}(t) = V_L(t).I_{cap}(t) \tag{7}$$

$$\dot{V}_{cap}(t) = -\frac{1}{C} I_{cap}(t) \tag{8}$$

$$SOC(t) = \frac{Q(t)}{Q_{\max}} = \frac{CV_{cap}(t)}{CV_{\max}} = \frac{V_{cap}(t)}{V_{\max}} \tag{9}$$

$$SOE(t) = \frac{E(t)}{E_{cap}} = \frac{\frac{1}{2}CV_{cap}(t)^2}{\frac{1}{2}CV_{\max}{}^2} = \frac{V_{cap}(t)^2}{V_{\max}{}^2} = SOC(t)^2 \tag{10}$$

where P_{uc} is the output power of the ultracapacitor; V_L is the voltage at the terminals; I_{cap} is the current; V_{cap} is the voltage across the equivalent capacitance; $V_{\max}$ is the maximum voltage of the ultracapacitor; C is the equivalent capacitance of the ultracapacitor pack; *SOC* is the state of charge defined as the amount of charge stored in the capacitance Q (t) relative to the maximum acceptable value $Q_{\max}$; *SOE* is the state of energy represents the amount of energy stored in the capacitance E (t) relative to maximum energy capacity E_{cap}.

The state of energy is also relative to the maximum energy capacity and is related to the integral of the power, as shown in (11). Since the problem is set up using power balance equations, it is more natural to use the state of energy of the ultracapacitor as the most immediate control variable for the HETB. The variation of the *SOE* with respect to time is expressed using the following dynamic equation:

$$\dot{SOE}(t) = \begin{cases} -\dfrac{1}{\eta_{cap}} \dfrac{P_{uc}(t)}{E_{cap}} & if\ P_{uc}(t) \ge 0\ \ (disch\arg e) \\ -\eta_{cap} \dfrac{P_{uc}(t)}{E_{cap}} & if\ P_{uc}(t) < 0\ \ (ch\arg e) \end{cases} \tag{11}$$

where η_{cap} is the ultracapacitor's efficiency.

The power balance model is adopted here to illustrate the relationship of the power from the genset, the ultracapacitor, and the electric motor, shown as:

$$P_{uc} = P_{gen,e} + P_{req} \tag{12}$$

$$P_e = \frac{P_{gen,e}}{\eta_g} = \frac{P_{uc} - P_{req}}{\eta_g} \tag{13}$$

where $P_{gen,e}$ is the electric power from the genset; P_{req} represents the power requirements for the powertrain; and η_g is the efficiency of the generator.

From (12), the following constraints on the ultracapacitor power are derived:

$$P_{req}(t) - P_{gen,e,\max} \le P_{uc}(t) \le P_{req}(t) - P_{gen,e,\min} \tag{14}$$

which must be satisfied together with the physical constraints:

$$P_{uc,\min}(t) \le P_{uc}(t) \le P_{uc,\max}(t) \tag{15}$$

In addition to this, the state of energy must remain within upper and lower boundary values:

$$SOE_{\min} \le SOE(t) \le SOE_{\max} \tag{16}$$

where $P_{gen,e,\max}$ and $P_{gen,e,\min}$ are the maximum and minimum electric power from the genset, respectively; $P_{uc,\max}$ and $P_{uc,\min}$ are the maximum and minimum output power of ultracapacitor, respectively; $SOE_{\max}$ is the maximum state of energy; and $SOE_{\min}$ is the minimum state of energy.

III. DYNAMIC PROGRAMMING FOR HETB

Differing from the rule-based strategy, the DP algorithm usually depends on a model to provide a provably optimal control strategy by searching all state and control grids exhaustively [23], [24]. However, the DP-based approach is not suitable for real-time application since the exact future driving information is seldom known in the real world [25]. Nonetheless, the DP-based strategy can provide a good benchmark to evaluate the optimality of other algorithms and contribute to perfect the real-time strategies [26], [27], [28].

DP breaks the optimization problem into a sequence of decision steps over time, and the optimization target is to minimize its cost function $J(x, u)$. The state of the system can be discretized into the state grid. At time step t_k, the system state x_k can be driven by control input u_k into another state at the next time instant t_{k+1}. The one step cost from t_k to t_{k+1} is defined as $J_{k\to k+1}$ and the accumulated cost from time step t_k to t_M is defined as $J_k = J_{k\to k+1} + J^*_{k+1}$. J^*_{k+1} represents the optimal accumulated cost from t_{k+1} to t_M. The goal of the DP algorithm is to calculate the optimal control inputs u_k^* that provide the minimum value of J_k at every time step k so that the state trajectory from every initial point will be guaranteed to be optimal. This procedure is performed through an iterative backwards optimization. The resulting u_k^* is saved as a function dependent on x_k.

The problem setup for the DP-based strategy requires discrete values of the control variable and a discrete-time description of the system. The procedure is implemented as follows.

A. Problem Formulation

The state and the control variables need to be determined in order to formulate the DP. As previously mentioned, the state is *SOE*. The control input refers to the power output of the ultracapacitor. The discrete-time model of the HETB can be expressed as:

$$x(k+1) = f(x(k), u(k)) \tag{17}$$

In the above equation, $u(k)$ and $x(k)$ are the control inputs and the state variables, respectively. The sampling time is chosen as 1 second. The vectors of states, control inputs, and measured inputs are defined as:

$$x = \begin{bmatrix} SOE \\ B_e \end{bmatrix}, u = P_{uc}, v = P_{req} \tag{18}$$

The linearized and discretized model of the system becomes:

$$x(k+1) = A(k)x(k) + B_u(k)u(k) + B_v(k) \tag{19}$$

In this equation,

$$A = \begin{bmatrix} 1 & 0 \\ 0 & 1 \end{bmatrix}; B_u(k) = \begin{bmatrix} -\dfrac{1}{E_{cap}} \\ -m_1 \end{bmatrix}; B_v(k) = \begin{bmatrix} 0 \\ m_1 * P_{ref} + m_2 \end{bmatrix};$$

The purpose of this optimization problem is to obtain the optimal control sequence, $u(k)$, and minimize the fuel consumption over a given drive cycle. The cost function of this optimization problem is described as follows:

$$J = \sum_{k=0}^{M-1} L(x(k), u(k)) \tag{20}$$

where, L refers to the instantaneous cost value (fuel consumption).

The physical constraints of state and control variables are denoted by the following inequalities to guarantee smooth/safe operation of the key components, including the engine, motor, and ultracapacitor:

$$\begin{cases} SOC_{\min} \le SOC \le SOC_{\max}; \\ SOE_{\min} \le SOE \le SOE_{\max}; \\ N_{e_\min} \le N_e \le N_{e_\max}; \\ P_{e_\min} \le P_e \le P_{e_\max}; \\ T_{e_\min} \le T_e \le T_{e_\max}; \end{cases} \tag{21}$$

Furthermore, the equality constraints are used such that the HETB can satisfy the load and speed requirements at all times.

B. Implementing Dynamic Programming

The main merit of the DP is that it is able to deal with the nonlinearity of the problem and the constraints while obtaining the optimal policy. The DP problem can be described by (22) and (23):

Step M-1:

$$J^*_{M-1}(x(M-1)) = \min_{u(M-1)} \left[L(x(M-1), u(M-1)) \right] \tag{22}$$

Step k, for $0 \le k < M-1$:

$$J^*_k(x(k)) = \min_{u(k)} \left[L(x(k), u(k)) + J^*_{k+1}(x(k+1)) \right] \tag{23}$$

where $J_k^*(x(k))$ refers to the optimal accumulated cost from time step t_k to the terminal; whereas, $x(k+1)$ means the state at the $(k+1)$th stage when the control variable u_k is applied at the time step t_k according to (19).

The optimal control policy is obtained by solving the above recursive equation backwards. The minimizations are conducted subject to the equality constraints imposed by the drive cycle and the inequality constraints shown in (21).

C. Procedure of Dynamic Programming

DP's procedure can be explained with the example shown in Fig.3, which refers to a generic HETB configuration with a single degree of freedom. The decision variable is the UC state of energy SOE, which can take a finite number of values (in the example, just three: 0.6, 0.65 or 0.7). The objective of the dynamic programming algorithm is to select the optimal sequence of SOE such that the total cost is minimized. Selecting a sequence of SOE is equivalent to deciding a sequence of values of UC power because the variation of SOE between time steps is proportional to the integral of the battery power between those steps.

The *SOE* (and not the power) is chosen as the decision variable because this allows us to satisfy the constraints on the maximum and minimum state of energy very easily since only the admissible values are considered; also, the initial and final values of the *SOE* are set with no effort. The constraints on the battery power are expressed in terms of maximum and minimum variation of *SOE* between two subsequent time steps.

The first step in applying the algorithm is calculating all the arc costs. These are the costs of moving from all admissible nodes at time k to all the admissible nodes at time $k+1$. Fig. a shows all the admissible arc costs in this case: for example, at time $k = N - 1 = 4$, all three values of the *SOE* are admissible (nodes *H*, *I*, *K*), but only one is accepted at the final time (node *L*); thus, three arc costs must be defined ($H \to L, I \to L$ and $K \to L$). At time $k = 3$, however, there are nine possible combinations (from any of the nodes *E*, *F, G* to any of the nodes *H*, *I*, *K*). Similar considerations can be made for all other time steps. Once all the arc costs have been determined, the cost-to-go can be calculated, starting from the final point and going backwards (Fig.b). At time $k = 4$, the cost-to-go of each node *H*, *I, K* corresponds to the arc cost because the following time instant is the end of the optimization horizon. At time $k = 3$, the cost-to-go of each node corresponds to the minimum cost associated with moving from that node to the end. Thus, for node *E*, the cost-to-go is the one corresponding to path with minimum cost among the possible alternatives: $E \to H \to L$, $E \to I \to L$, and $E \to K \to L$. The respective costs are (from Fig.a): 2+1.4=3.4, 2.3+1.9=4.2, and 1.8+0.7=2.5; these values are shown in Fig.b in correspondence with the respective path. Thus, the best path from *E* to *L* passes through *K* and has a cost of 2.5; the best path from *F* to *L* passes through *K* and has a cost of 1.6, and the best path from *G* to *L* passes through *H* and has a cost of 1.4. This is all the information needed before the algorithm moves to the preceding time step ($k = 2$), and computes the arc costs for points *B*, *C*, and *D*. Because of Bellman's optimality principle, the optimal path from *E*, *F*, or *G* to *L* is not affected by the

choice at the previous time step, therefore, the cost-to-go from B to L is given by the sum of the arc cost from B to either E, F, G and the optimal cost from there to L: for example, going from B to L passing through E costs 1.9 (cost of $B \to E$) plus 2.5 (lowest cost of $E \to L$). With similar reasoning, the entire graph of Fig.b is completed with the arc costs, and it isthen possible to choose the optimal path as the one with the lowest cost from A to L. This is 4.9 and is obtained passing through B, F and K.

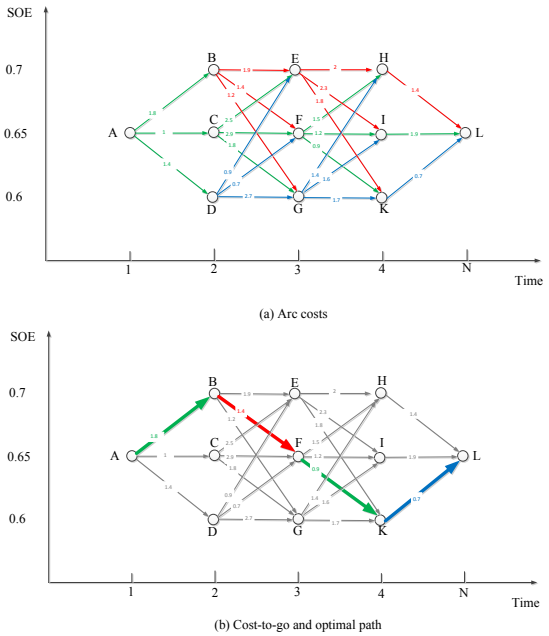

Fig.3 Application of dynamic programming to the HETB

IV. Case Study

In this section, the comparison between the results from the aforementioned energy management strategy and the rule-based strategy are conducted and discussed in two scenarios. The first scenario is under a typical drive cycle. Secondly, with the preliminary knowledge of the typical drive cycle, the DP is tested under a drive cycle with 40% disturbances to evaluate the robustness of the proposed method. In this article, the rule-based control strategy was implemented as follows: the engine output power follows the load demand power of the bulldozer, and the ultracapacitor supplements the power shortage caused by the excessive load demand power as the auxiliary power source.

A. Scenario 1: Typical drive cycle

In this scenario, the typical working condition is used for the simulation. In Fig. 4, velocity (km/h) is the bulldozer velocity and the depth (m) is soil-cut depth. The working stages are described as follows: 1~4-s is the traveling stage; 4~16-s is the soil-cutting stage; 16~31-s is the soil-transportation stage; 31~33-s is the unloading soil stage, and 33~50-s is the no-load stage. Fig.5 shows the power demand calculated according to the typical working condition by the equations described in Section II.

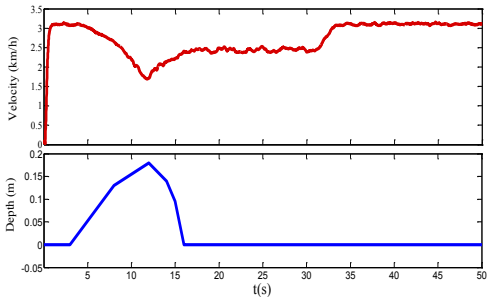

Fig.4 Typical working condition of HETB

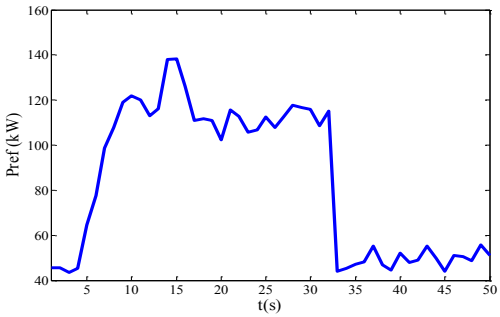

Fig.5 Power demand of the typical working condition

The engine and ultracapacitor output power and the variation of the *SOE* for the DP are presented in Fig. 6 and Fig. 7.

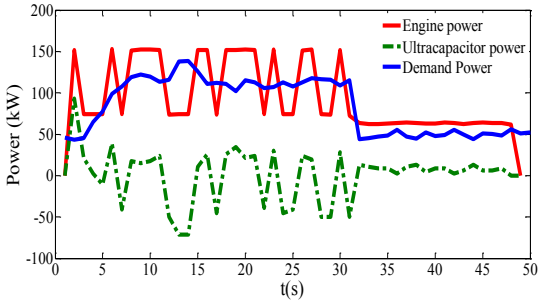

Fig.6 Dynamic programming results under scenarios 1

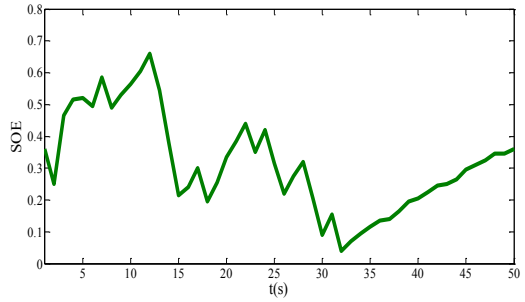

Fig.7 Power demand of the typical working condition

In order to demonstrate the advantage of the hybrid configuration as well as the DP strategy's application, the fuel consumption in different cases is provided in Table I. The fuel consumption of the rule-based strategy is 310g. To compensate for the *SOE* difference between the initial and final values, the correction method proposed in [29] is used such that the comparison can be performed. The DP strategy can improve

TABLE I
FUEL CONSUMPTION COMPARISON UNDER SCENARIO 1

Control Strategy	Fuel Consumption (g)	Fuel Economy (%)
DP	290	7%
Rule-based	313	---

fuel economy by 7%.

B. Scenario 2: A Combined drive cycle

In order to verify the robustness of the proposed DP method, 40% disturbances are added to the typical working condition as shown in Fig.8. The engine and ultracapacitor output power and the variation of the *SOE* for the DP are presented in Fig. 9 and Fig. 10. The fuel consumption of the rule-based strategy is 334.8g. The DP strategy can improve fuel economy by 9%.

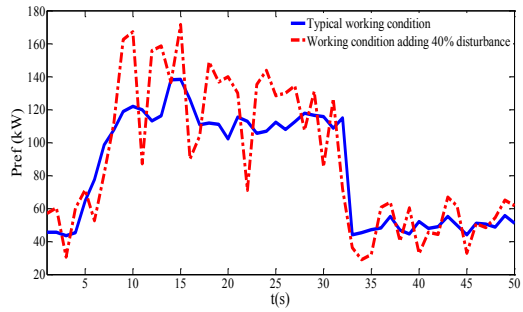

Fig.8. Power demand comparison under scenario 2

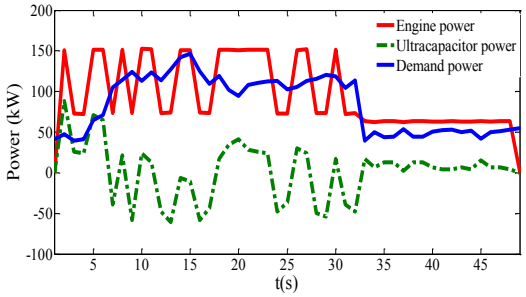

Fig.9. Dynamic programming results under scenario 2

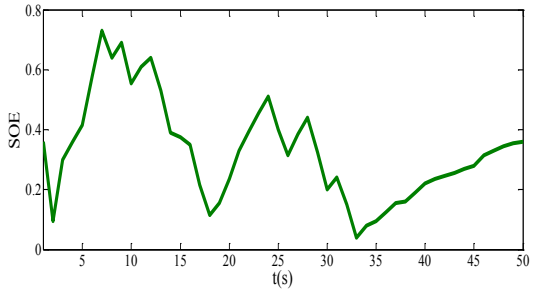

Fig.10. SOE profile comparison under scenario 2

TABLE II
FUEL CONSUMPTION COMPARISON IN SCENARIO 2

Control Strategy	Final SOE	Fuel Consumption (g)	Fuel Economy (%)
DP	0.36	304.7	9%
Rule-based	0.34	334.8	---

V. CONCLUSIONS

The goal of this study was to develop a power management strategy without knowledge of future driving information for the HETB. A DP power management strategy was introduced based on averaged power information. HETBs with different strategies were simulated for two cases. In the first case, the typical drive cycle was used to find and tune controller parameters. Then, in order to verify the robustness of the proposed strategy under large disturbances, a 40% stochastic disturbance was added to the typical drive cycle. The results demonstrated that the proposed method can provide a 7%-9% fuel economy improvement than that of rule-based strategy.

ACKNOWLEDGEMENT

The authors would like to appreciate the financial support of the Natural Sciences and Engineering Research Council of Canada (NSERC) and the Ontario Research Fund.

References

[1] H. A. Borhan, A. Vahidi, A. M. Phillips, M. L. Kuang, and I. V. Kolmanovsky, “Predictive energy management of a power-split hybrid electric vehicle,” in Proc. Amer. Control Conf. (ACC), Jun. 2009, pp.3970-3976.

[2] C. C. Lin, H. Peng, J.W. Grizzle, and J. M .Kang, “ Power management strategy for a parallel hybrid electric truck,” IEEE, Trans. Contr. Syst. Technol., vol.11, pp. 839-843, Nov. 2003.

[3] A. Sciarretta, and L. Guzzella, “Control of hybrid electric vehicles,” IEEE Control System Magazine, pp. 60-70, April 2007.

[4] R. Wang, and S. M. Lukic, “Dynamic programming technique in hybrid electric vehicle optimization,” Electric Vehicle Conference (IEVC), 2012 IEEE International, Mar. 2012, pp. 1-8.

[5] Huang, Yanjun, et al. "Model predictive control power management strategies for HEVs: A review." *Journal of Power Sources* 341 (2017): 91-106.

[6] K. Ç. Bayindir, M. A. Gözüküçük, and A. Teke, “A comprehensive overview of hybrid electric vehicle: Powertrain configurations, powertrain control techniques and electronic control units,” Energy Convers. Manage. , vol. 52, no. 2, pp. 1305–1313, Feb. 2011.

[7] Wang, H., Huang, Y., Khajepour, A., & Song, Q. "Model predictive control-based energy management strategy for a series hybrid electric tracked vehicle." Applied Energy 182 (2016): 105-114.

[8] T. Qu, H.Chen, D. P. Cao, H. Y. Guo, and B. Gao, “Switching-based stochastic model predictive control approach for modeling driver steering skill,” IEEE, Trans. on Intelligent Transportation Systems, vol. 16, pp. 365-375, Feb. 2015.

[9] C. Vagg, S. Akehurst, C. J. Brace, and L. Ash, “Stochastic dynamic programming in the real-world control of hybrid electric vehicles,” IEEE, Trans. Contr. Syst. Technol., vol. PP, pp. 1-14, Nov. 2015.

[10] K. Xu, B. Qiu, G. Liu, and Q. S. Chen, “Energy management strategy design of plug-in hybrid electric bus based on pontryagin’s minimum principle,” ITEC Asia-Pacific, SEP. 2014, pp.1-6.

[11] G. Paganelli, T. Guerra, S. Delprat, J. Santin, M. Delhom, and E. Combes, “ Simulation and assessment of power control strategies for a parallel hybrid car,” Proceedings of the Institution of Mechanical Engineers, Part D: Journal of Automobile Engineering, vol. 214, no.7, pp. 705-717, 2000.

[12] L. Serrao, S. Onori, and G. Rizzoni, “ECMS as a realization of Pontryagin’s minimum principle for HEV control,” in Proc. Amer. Control Conf. (ACC), Jun. 2009, pp. 3964–3969.

[13] N. Kim, S. Cha, and H. Peng, “Optimal control of hybrid electric vehicles based on Pontryagin’s minimum principle,” IEEE Trans. Control Syst. Technol., vol. 19, no. 5, pp. 1279–1287, Sep. 2011.

[14] B. M. Baumann, G. N. Washington, B. C. Glenn, and G. Rizzoni, “Mechatronic design and control of hybrid electric vehicles,” IEEE/ASME Trans. Mechatron., vol. 5, pp. 58-72, 2000.

[15] N. Schouten, M. Salman, and N. Kheir, “Fuzzy logic control for parallel hybrid vehicles,” IEEE, Trans. Contr. Syst. Technol., vol. 10, pp. 460-468, May 2002.

[16] L. V. Pérez, G. R. Bossio, D. Moitre, and G. O. García, “Optimization of power management in an hybrid electric vehicle using dynamic programming,” Math. Comput. Simul., vol. 73, nos. 1–4, pp. 244–254, Nov. 2006.

[17] Huang, Y., Khajepour, A., Wang, H. " A Predictive Power Management Controller for Service Vehicle Anti-idling Systems without a priori Knowledge of Future Driving." Applied Energy , Doi: 10.1016/j.apenergy.2016.08.143.

[18] J. Ribau, R. Viegas, A. Angelino, A. Moutinho, and C. Sliva, “A new offline optimization approach for designing a fuel cell hybrid bus,” Trans. Res. Part C: Emerg. Technol., vol. 42, pp. 14-25, May 2014.

[19] H. W. He, H. L. Tang, and X. M. Wang, “Global optimal energy management strategy research for a plug-in series-parallel hybrid electric bus by using dynamic programming,” Math. Probl. Eng., vol. 2013, doi:10.1155/2013/708261.
[20] L. Lai, and M. Ehsani, “Dynamic programming optimized constrained engine on and off control strategy for parallel HEV,” in Proceedings of the IEEE Vehicle Power and Propulsion Conference(VPPC), Beijing, China, Nov. 2012, pp.595-613.
[21] H. Wang, Q. Song, S. B. Wang, and P. Zeng, “ Dynamic Modeling and Control Strategy Optimization for a Hybrid Electric Tracked Vehicle, ” Math. Probl. Eng., vol. 2015, doi:10.1155/2015/251906.
[22] Bekker M G. Off-Road Locomotion. The Univ. of Michigan Press, Ann Arbor, Michigan, 1960.
[23] He, Hongwen, et al. "Energy management strategy research on a hybrid power system by hardware-in-loop experiments." Applied Energy 112 (2013): 1311-1317.
[24] Wang, X. M., He, H. W., Sun, F. C., Zhang, J. L, “Application study on the dynamic programming algorithm for energy management of plug-in hybrid electric vehicles,” Energies, vol.8, pp. 3225-3244, 2015.
[25] S. Kermani, S. Delprat, T. M. Guerra, R. Trigui, B. Jeanneret, “Predictive energy management for hybrid vehicle,” Control Eng. Pract. , vol. 20, pp. 408-420, Apr. 2012.
[26] J. Ribau, R. Viegas, A. Angelino, A. Moutinho, and C. Sliva, “A new offline optimization approach for designing a fuel cell hybrid bus,” Trans. Res. Part C: Emerg. Technol., vol. 42, pp. 14-25, May 2014.
[27] H. W. He, H. L. Tang, and X. M. Wang, “Global optimal energy management strategy research for a plug-in series-parallel hybrid electric bus by using dynamic programming,” Math. Probl. Eng., vol. 2013, doi:10.1155/2013/708261.
[28] L. Lai, and M. Ehsani, “Dynamic programming optimized constrained engine on and off control strategy for parallel HEV,” in Proceedings of the IEEE Vehicle Power and Propulsion Conference(VPPC), Beijing, China, Nov. 2012, pp.595-613.
[29] Zhang, C. G., Zeng, K. H., Zhao, J. H, "Analytical Solutions of Critical Load and Terzaghi’s Ultimate Bearing Capacity for Unsaturated Soil," Journal of tongji university (natural science), vol. 38, pp. 1736-1739,2010.

Contact information

Dr. Hong Wang
Department of Mechanical and Mechatronics Engineering,
University of Waterloo, Ontario, N2L3G1, Canada
H492wang@uwaterloo.ca

Dr. Yanjun Huang
Department of Mechanical and Mechatronics Engineering,
University of Waterloo, Ontario, N2L3G1, Canada
y269huan@uwaterloo.ca

Dr. Chen Lv
Advanced Vehicle Engineering Centre, Cranfield University
Cranfiled, MK43 0AL, United Kingdom
C.Lyu@cranfield.ac.uk

Dr. Amir Khajepour
Department of Mechanical and Mechatronics Engineering,
University of Waterloo, Ontario, N2L3G1, Canada
a.khajepour@uwaterloo.ca

https://dspace.org/

Global optimal energy management strategy research for hybrid electric off-road vehicles

Wang, Hong; Huang, Yanjun; Lv, Chen; Khajepour, Amir

2017-03-28
Society of Automotive Engineers (SAE)
https://saemobilus.sae.org/content/2017-01-0425
Wang H, Huang Y, Lv C, Khajepour A. (2017) Global optimal energy management strategy research for hybrid electric off-road vehicles. SAE International Journal of Commercial Vehicles, Volume 10, Issue 2, pp. 524-531, SAE 2017-01-0425

Downloaded from a DSpace repository. https://dspace.org/